Talanta 115 (2013) 512–517

Contents lists available at SciVerse ScienceDirect

Talanta

journal homepage: www.elsevier.com/locate/talanta

Nanocomposite-based rapid, visual, and selective luminescence turn-on assay for Hg^{2+} sensing in aqueous media

Jiabin Cui, Mingyue An, Leyu Wang*

State Key Laboratory of Chemical Resource Engineering, School of Science, Beijing University of Chemical Technology, Beijing 100029, China

ARTICLE INFO

Article history:
Received 2 April 2013
Received in revised form
28 May 2013
Accepted 30 May 2013
Available online 7 June 2013

Keywords:
Luminescence turn-on
Mercury detection
Nanocomposites

ABSTRACT

Composite nanospheres containing dithizone, luminescent $LaVO_4:Eu^{3+}$ nanoparticles (NPs), and amphiphilic polymer have been composed for the rapid, selective, and visual luminescence turn-on detection of mercury ions (Hg^{2+}) in water. Due to the absorption of dithizone, the strong red luminescence of $LaVO_4:Eu^{3+}$ NPs encapsulated in nanospheres was quenched noticeably. As a result, these as-prepared nanocomposites (NCs) demonstrate very weak red luminescence. However, in the presence of Hg^{2+}, the red luminescence of nanocomposites was turned on dramatically, which can be attributed to the strong binding of mercury (II) ions by dithizone and forming a complex without absorption in the red emission range. Meanwhile, other cations have no influence on the detection of Hg^{2+}, suggesting a good selectivity for Hg^{2+} sensing. Due to the high photostability and chemical stability of the nanocomposites, operation simplicity, low cost, and good selectivity, this newly developed method is highly desirable for field assay of Hg^{2+} in aqueous media ranging from 40.0 nM to 4.0 μM with a limit of detection of 32.0 nM and a good linearity (r=0.9980). Therefore, a facile, rapid, selective, and visual luminescence turn-on technology has been successfully developed for Hg^{2+} detection.

1. Introduction

Developments of universal protocols for the selective, visual, and field detection of mercury (II) ions contamination in aquatic ecosystems have attracted much interest due to the increasing threat of heavy metal contamination to the environment and the severe effects on human health [1–5]. According to the Environmental Protection Agency (EPA), coal-burning power plants are the largest human-caused sources of Hg emission to the air. Once released into air, Hg eventually settles into water or onto land where it is washed [6–14]. Exposure to high Hg levels can harm the brain, heart, kidneys, lungs, and immune system of people of all ages, so it is important for monitoring Hg levels in the aquatic ecosystem as a potential source of contamination. So far, several methods, such as atomic absorption spectroscopy, gas-chromatography inductively coupled with plasma-mass spectrometry (GC–ICP-MS), atomic fluorescence spectrometry (AFS), inductively coupled with plasma-atomic emission spectrometry (ICP-AES), and reversed-phase high-performance liquid chromatography (HPLC) have been developed to monitor the concentration of Hg^{2+} in water samples [15–18]. Their excellent performance, however, is achieved at the expenses of expensive instruments, elaborate and time-consuming sample preparations and preconcentration procedures [19–35], which usually limit the field application. Recently, oligonucleotide-based fluorescence probe through the specific T–Hg^{2+}–T (T=thymine) binding for mercury detection has also drawn great attention [36–43]. But these fluorescence probes are mainly based on the organic dyes that usually suffer from photobleaching. It is still a challenge to develop a simple, efficient, low-cost, and suitable in-situ visual detection of Hg^{2+} ions in aqueous media.

Herein, we developed a facile strategy to fabricate the nanoplatform for visual and field Hg^{2+} luminescence turn-on detection independent of complicated sample pre-treatment and expensive instruments. Briefly, a novel and facile approach has been developed to fabricate the water-dispersible and functional $LaVO_4:Eu^{3+}$–dithizone nanocomposites. As shown in Scheme 1, the hydrophobic $LaVO^4:Eu^{3+}$ NPs [44–47] and hydrophobic dithizone [48–53] were encapsulated into a hydrophilic polymer nanosphere (Scheme 1A) [54–57]. These composite nanospheres are highly water-stable but no red luminescence (620 nm) of $LaVO_4:Eu^{3+}$ NPs was observed due to the dramatic quenching by dithizone whose absorption peak is centered at 610 nm. However, in the presence of Hg^{2+}, dithizone (D) formed the D–Hg^{2+}–D complex due to its strong chelating ability to Hg^{2+}, and the absorption peak of D–Hg^{2+}–D complex blue-shifts to 502 nm from 610 nm and consequently (Fig. S1), the red luminescence of nanocomposites is turned on (Scheme 1B). Therefore, a novel and facile luminescence turn-on strategy was successfully

* Corresponding author. Tel./fax: +86 10 6442 7869.
E-mail address: lywang@mail.buct.edu.cn (L. Wang).

0039-9140/$ - see front matter © 2013 Elsevier B.V. All rights reserved.
http://dx.doi.org/10.1016/j.talanta.2013.05.069

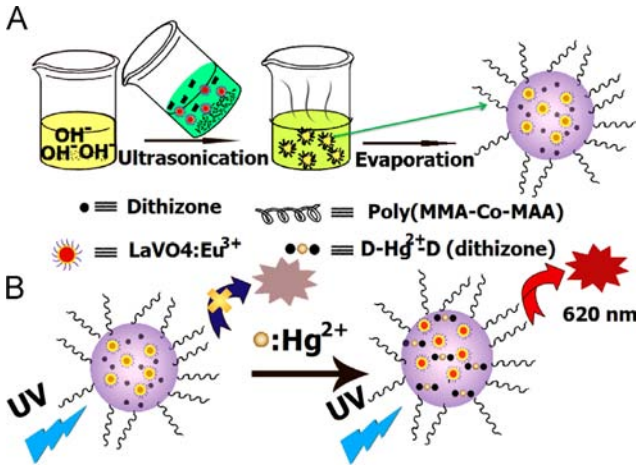

Scheme 1. Schematic diagram of (A) synthesis of nanocomposites and (B) luminescence turn-on detection for Hg^{2+} based on the nanocomposites.

developed for the selective detection of mercury (II) ions. [31,33,55–64].

2. Experimental section

2.1. Regents and materials

Oleic acid was obtained from Alfa. NH_4VO_3 was from Tianjin Fuchen Chemicals Co. (Tianjin, China). $La(NO_3)_3 \cdot 6H_2O$ and $Eu(NO_3)_3 \cdot 6H_2O$ were purchased from Beijing Ouhe Chemical Reagent Company. The monomers, methacrylic acid (MAA) as well as methyl methacrylate (MMA), and azoinitiator 2,2′-azobisisobutyronitrile (AIBN) were obtained from Tianjin Chemical Factory (China). NaOH, ethanol, dithizone, cyclohexane, chloroform and methanol, $CaCl_2$, $CoCl_2 \cdot 6H_2O$, $FeCl_3 \cdot 6H_2O$, $HgCl_2$, KBr, $NaH_2PO_4 \cdot 2H_2O$, Na_2HPO_4, NaCl, $ZnCl_2$, $MnCl_2$, $CdCl_2 \cdot 2.5H_2O$, $Pb(NO_3)_2$, $MgCl_2 \cdot 6H_2O$, $NiCl_2 \cdot 6H_2O$, $CuSO_4 \cdot 5H_2O$, $Al(NO_3)_3 \cdot 9H_2O$, $AgNO_3$, and NH_4Cl were obtained from Beijing Chemical Reagent Company. All reagents are analytical grade and used as received without further purification. Deionized (DI) water was used throughout.

2.2. Characterization

Transmission electron microscope (TEM) images were obtained on a Hitachi H-800 transmission electron microscope operated at 200 KeV. Optical properties of the NPs were characterized using a Hitachi F-4600 fluorescence spectrophotometer equipped with a plotter unit and a quartz cell (1 cm × 1 cm).

2.3. Synthesis of luminescent $LaVO_4:Eu^{3+}$ nanocrystals

Luminescent $LaVO_4:Eu^{3+}$ nanoparticles (NPs) were prepared according to the reported method with minor alteration [56,65]. In brief, NH_4VO_3 (0.06 g) and NaOH (0.6 g) were first dissolved in DI water (5 mL) followed by the addition of ethanol (10 mL) and oleic acid (10 mL). Finally, 1 mL of the mixed solution (total $[Re^{3+}]$= 1.0 M) of $La(NO_3)_3$ and $Eu(NO_3)_3$ (La^{3+}/Eu^{3+}=98/2) was added. The mixture was stirred thoroughly and then transferred into a Teflon-lined autoclave. Thereafter the autoclave was heated at 140 °C for 5 h and then cooled to room temperature. The product deposited onto the bottom of the autoclave was collected and washed with cyclohexane. The obtained white products were then dispersed in chloroform (4 mL) and stored for later use.

2.4. Synthesis of poly(MMA-co-MAA).

In a typical synthesis of the copolymer methyl methacrylate-co-methacrylic acid (poly(MMA-co-MAA)), 0.2 g MAA, 4.6 g MMA and 0.096 g AIBN were mixed in 35 mL of chloroform solution. The mixture was then transferred into a 40 mL Teflon-lined vessel, sealed in an autoclave, and then treated for about 10 h at 100 °C. After the autoclave was allowed to cool to room temperature naturally, the products could be collected via precipitation in methanol. The copolymers were further purified by dissolving them in 10 mL of chloroform, precipitating by the addition of methanol (100 mL), and collecting via centrifugation. The final products were obtained after two cycles of purification.

2.5. Preparation of nanocomposites

In a typical procedure, 30 mg of the as-synthesized poly(MMA-co-MAA) was first dissolved in chloroform (0.5 mL) followed by the addition of luminescent NPs (20 mg) as well as dithizone (1.0 mg), and then the mixture solution was diluted to 1.0 mL with chloroform. Thereafter, the mixture solution was transferred into 10 mL of NaOH aqueous solution (70 μg/mL) under vigorous stirring and ultrasonic treatment, and the dark green emulsion was subsequently obtained. This emulsion was then stirred at 60 °C for 2 h to remove the chloroform. The composite nanospheres were collected by centrifugation and redispersed in 5.0 mL deionized (DI) water and stored for use. Other nanocomposites with various amount of dithizone were prepared via the same protocol except for different dithizone dose.

2.6. Luminescence turn-on detection of Hg^{2+}

Briefly, into a 1.5 mL vial, 50 μL of nanocomposite colloidal solution (0.5 mg/mL), and a given concentration of Hg^{2+} standard solution were added. Finally the mixture solution was diluted to 1.0 mL with PBS (0.02 M, pH=7.0), mixed thoroughly and incubated at 45 °C for 20 min. The luminescence enhancement effects were carried out with the excitation and emission wavelength of 254 nm and 620 nm, respectively.

3. Results and discussion

The morphology and size distribution of these nanocomposites were observed by transmission electron microscope (TEM). From the TEM images shown in Fig. 1, it can be seen that the as-prepared nanocomposites are sphere in shape with an average size of 400 nm. Meanwhile, the luminescent $LaVO_4:Eu^{3+}$ inorganic NPs are embedded in the polymer matrixes with the observable rodlike dots. Actually, the rodlike dots are $LaVO_4:Eu^{3+}$ nanoplates in the side view (Fig. 1a–d) [65,66]. High magnification TEM image of the composite nanosphere clearly demonstrated the plate shape of $LaVO_4:Eu^{3+}$ (Fig. 1e). Meanwhile, the TEM image of hydrophobic $LaVO_4:Eu^{3+}$ nanoplates was shown in Fig. 1f. The influence of dithizone dosage on the shape and size of nanocomposites was also investigated. By increasing the dithizone content from 1.0 mg (Fig. 1a) to 1.5 mg (Fig. 1b) and then 2.0 mg (Fig. 1c), the shape of nanocomposites had no obvious change but the size distribution became wider. Judging from the morphology, it is easy to find that the nanospheres with 1.0 mg dithizone are more homogeneous. We also investigated the fabrication of nanocomposites with lower content of dithizone. Although the shape and size of these nanospheres are better (Fig. S2), the luminescence of $LaVO_4:Eu^{3+}$ NPs embedded in the polymer matrixes could not be quenched efficiently by the limited dithizone, which is unfavorable for the luminescence turn-on analysis of Hg^{2+} ions. As a control, the

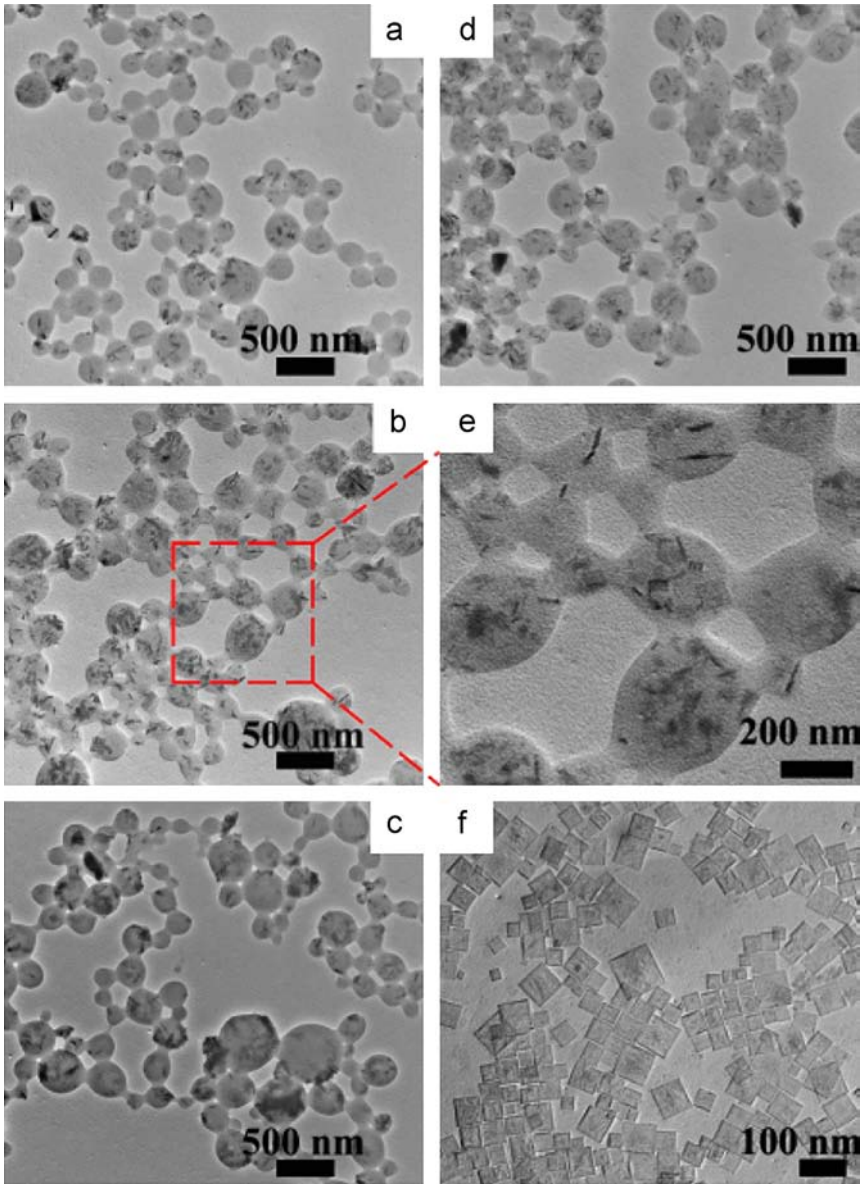

Fig. 1. TEM images of nanocomposites with low (a–d) and high (e) magnification of (b), and $LaVO_4$:Eu^{3+} NPs (f). Dosage of dithizone: (a), 1.0 mg; (b) and (e); 1.5 mg; (c), 2.0 mg; (d), 0.0 mg.

$LaVO_4$:Eu^{3+} NPs–polymer nanocomposites without dithizone were also fabricated (Fig. 1d). Compared with the dithizone doped nanocomposites, no obvious change in the shape and size of these nanocomposites without dithizone can be observed.

On the other hand, the influence of dithizone contents on the luminescence turn-off and turn-on of the nanocomposites was further investigated. As shown in the photoluminescence spectra of the nanocomposite colloidal solution (Fig. 2), the nanocomposites without dithizone doping show bright red luminescence (Fig. 2a). With the dose increase of doped dithizone from 1.0 to 2.0 mg, the red luminescence of the nanocomposites was quenched step by step and no red emission was observed from nanocomposites doped with 2.0 mg of dithizone (Fig. 2d). The luminescence quenching efficiency was noticeable with 2.0 mg of dithizone, however, it is hard to turn on the luminescence with the addition of mercury ions and consequently, not favorable for Hg^{2+} detection. Therefore, 1.0 mg of dithizone was chosen for the fabrication of the nanocomposites that were suitable for luminescence turn-on detection of Hg^{2+}.

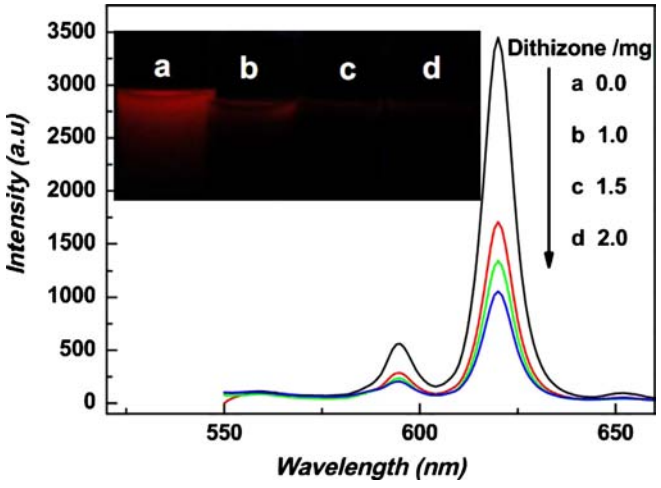

Fig. 2. Luminescence quenching efficiency with different contents of dithizone doped into the nanospheres. $\lambda_{em}/\lambda_{ex}$=620/254 nm.

As mentioned above, under excitation of 254 nm light, the nanocomposite colloidal solution emits weak red luminescence, but this emission is enhanced dramatically with the addition of mercury ions (Hg^{2+}). But the luminescence turn-on response speed was affected by the incubation temperature. Herein, at different incubation temperature, the kinetics of the Hg^{2+} recognition reaction was monitored by recording the luminescence intensity at 620 nm at different time. As shown in Fig. 3, in the presence of Hg^{2+}, the luminescence was enhanced dramatically to the highest point in 1 h at room temperature (25 °C) and then kept stable over at least 3 h. By increasing the temperature to 35 °C, the luminescence intensity reached the highest value in 35 min. Further increasing the temperature to 45 °C and 60 °C, only 20 min and 15 min, respectively were needed before the luminescence was enhanced to the summit and kept stable. For the convenience of field assays, the incubation temperature was set at 45 °C and the incubation time was 20 min in this work.

The pH influence on the reaction between nanocomposites and Hg^{2+} was also investigated. The results depicted in Fig. 4 demonstrated that the luminescence was enhanced at utmost and kept stable in the pH range of 7–9. Therefore, the detection of Hg^{2+} was conducted at pH=7 (PBS) after adding Hg^{2+} into the nanocomposite colloidal solution.

Detailed luminescence enhancement of nanocomposites with different concentration of Hg^{2+} (0–7.0 μM) is depicted in Fig. 5. In addition, the luminescence intensity (I) as a function to the concentration of Hg^{2+} has a good linear relationship in the range of 40.0–4.0 μM of Hg^{2+} with a limit of detection (LOD=$3\sigma/K$) of 32.0 nm. Herein, the σ is the standard deviation of the blank measurements (n=6), and the K is the slope of the calibration curve. A calibration function of I=1694.0+185.4C (μM) with a good linearity (r=0.9980) for the Hg^{2+} detection was obtained. Fig. S3 also depicted the true color luminescence photographs of the nanocomposite colloidal solution in the presence of different concentration of Hg^{2+}, suggesting these nanocomposites are capable of visual detection of Hg^{2+} ions. Therefore, a facile and sensitive luminescence turn-on nanosensor was successfully developed for the quantification of Hg^{2+} in aqueous media.

The selectivity of the nanocomposite luminescence turn-on assay has been evaluated by testing the luminescence response to coexisting cations such as $Ca^{2+}(Cl^-)$, $Zn^{2+}(Cl^-)$, $Pb^{2+}(NO^{3-})$, $Co^{2+}(Cl^-)$, $Cu^{2+}(SO_4^{2-})$, $Mn^{2+}(Cl^-)$, $Fe^{3+}(Cl^-)$, $Mg^{2+}(Cl^-)$, $Ni^{2+}(Cl^-)$, $Al^{3+}(NO^{3-})$, and $K^+(Br^-)$. As shown in Fig. 6a, Hg^{2+} can lead to dramatic luminescence enhancement. However, other ions do not influence the luminescence, except for only a slight luminescence enhancement by Mg^{2+}. At the same time, the experiment about interfering effects of sample matrixes at high level has been done and the concentration of coexisting cations was 20 times (100.0 μM) that of mercury ions (5.0 μM). As shown in Fig. S4, even at such a high concentration, only Pb^{2+}, Zn^{2+}, and Ni^{2+} ions have a slight interference and we can still easily distinguish mercury ions from other cations. In addition, the luminescence photographs of the nanocomposite colloidal solution with different cations were taken under UV lamp (254 nm) irradiation. As shown in Fig. 6b, before the addition of Hg^{2+}, no luminescence was observed from the nanocomposite colloidal solution. However, in the presence of Hg^{2+} (5.0 μM), the red luminescence was turned on obviously. In the cases of other cations, no red luminescence was observed, suggesting a very good selectivity for Hg^{2+} visual sensing. Therefore, the as-prepared nanocomposite can act as a selective luminescence turn-on probe for Hg^{2+} detection. The good selectivity is further verified through the study of the luminescence behavior in tap water, real water samples, and cell culture medium. As no mercury ions in the tap water and real water samples were

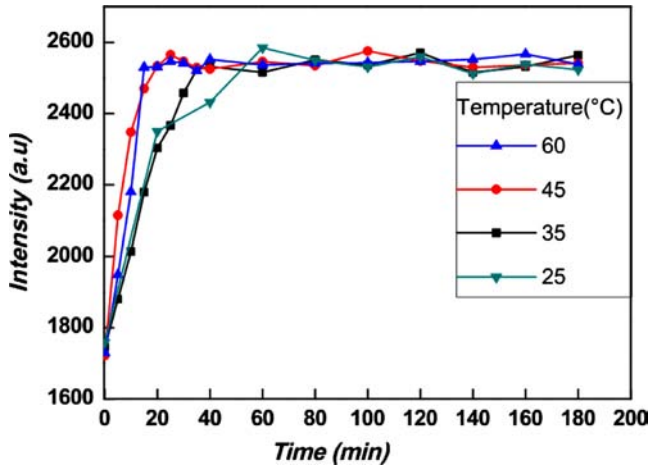

Fig. 3. Effects of incubation temperature and time on the luminescence intensity of nanocomposites (50 μg/mL) in the presence of Hg^{2+} (5.0 μM). $\lambda_{em}/\lambda_{ex}$=620/254 nm..

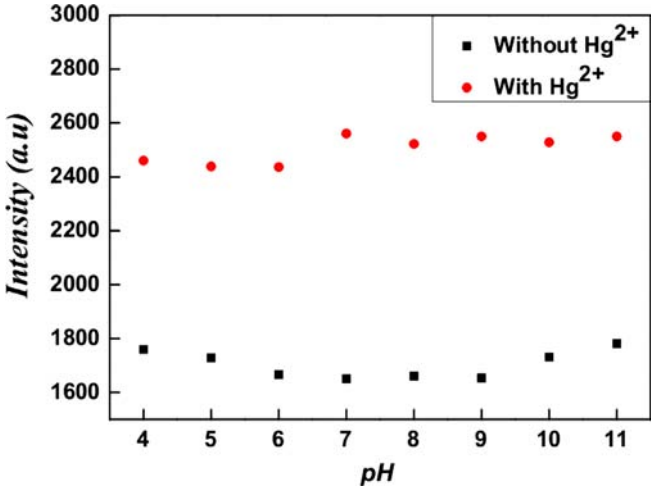

Fig. 4. Effects of pH value on the luminescence intensity of the nanocomposite (50 μg/mL) in the presence of Hg^{2+} (5.0 μM). $\lambda_{em}/\lambda_{ex}$=620/254 nm; Buffer solution and concentration, pH (4, 5): CH_3COOH–CH_3COONa (0.02 mol/L); pH (6–8): NaH_2PO_4–Na_2HPO_4 (0.02 mol/L); pH (9–11): Na_2CO_3–$NaHCO_3$ (0.02 mol/L).

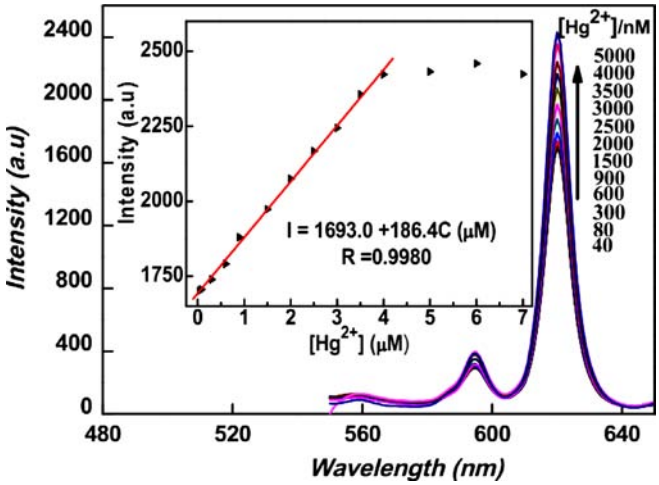

Fig. 5. Luminescence evolution of nanocomposites (50 μg/mL) in the presence of different concentration of Hg^{2+} (0–5.0 μM) in NaH_2PO_4–Na_2HPO_4 buffer solution (PBS, 0.02 M, pH=7.0). Inset: linear plot of luminescence enhancement of nanocomposites versus Hg^{2+} concentration (0–4.0 μM).

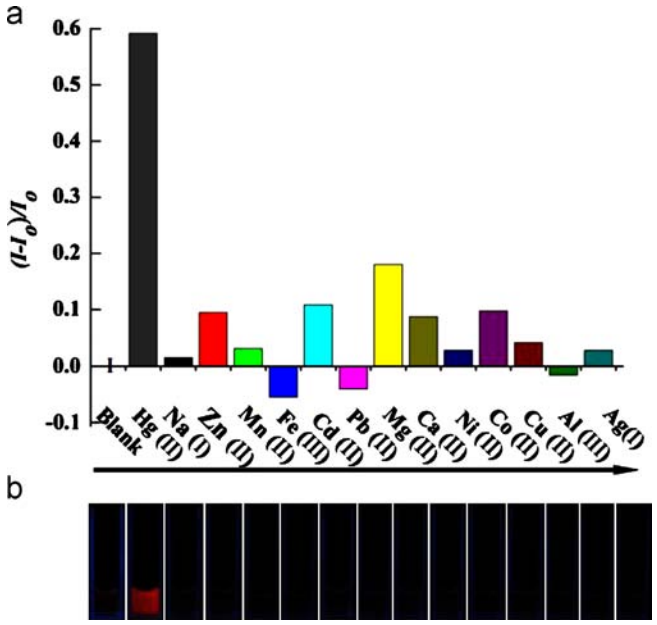

Fig. 6. Interference of coexisting cations on the luminescence of nanocomposites (50 μg/mL) in PBS (0.02 M, pH=7.0) (a) and luminescence photographs of the nanocomposite colloidal solution with different cations under UV lamp (254 nm) (b) Concentration of each cation was 5.0 μM.

Table 1
Analytical results for the detection of Hg^{2+} in tap water samples.[a]

Sample	Concentration (μM)		Recovery (%)
	Taken	Found (mean, $n=6$)	
Tap water	0.08	0.0756 ± 0.0015	94.4 ± 2.0
	0.8	0.8396 ± 0.0582	105 ± 6.9
	4.0	3.9812 ± 0.2557	99.5 ± 6.4

[a] n is the repetitive measurement number.

Table 2
Analytical results for the detection of Hg^{2+} in real water samples.[a]

sample	Concentration (μM)		Recovery (%)
	Taken	Found (mean, $n=6$)	
Lake water (Beijing)	4.0	3.9731 ± 0.2576	99.3 ± 6.5
River water (Tianjin)	4.0	4.0813 ± 0.1723	102 ± 4.2
River water (Shijiazhuang)	4.0	4.1756 ± 0.2342	104 ± 5.6

[a] n is the repetitive measurement number.

Table 3
Analytical results for the detection of Hg^{2+} in cell culture medium.[a]

Sample	Concentration (μM)		Recovery (%)
	taken	Found (mean, $n=6$)	
Cell culture medium	0.08	0.0912 ± 0.0082	114 ± 8.9
	0.8	0.8437 ± 0.0457	105 ± 5.5
	4.0	4.2763 ± 0.2597	107 ± 6.1

[a] n is the repetitive measurement number.

detectable through the proposed method, recovery studies were carried out on the tap water samples spiked with 80 nM, 0.8 μM, and 4.0 μM of Hg^{2+} and on the real water samples spiked with 4.0 μM of Hg^{2+}, respectively. At the same time, a recovery study was also carried out on the cell culture medium samples spiked with 80 nM, 0.8 μM, and 4.0 μM of Hg^{2+} to evaluate the developed method. As shown in Tables 1–3, the observations show a good recovery and potential applicability of this facile luminescence turn-on assay for Hg^{2+} in real samples.

4. Conclusions

In summary, via an ultrasonication-assisted assembly technology, hydrophobic dithizone (energy acceptors) and $LaVO_4:Eu^{3+}$ luminescence nanoparticles (energy donors) were simultaneously encapsulated into the hydrophilic polymer nanosphere. Due to the absorption peak of dithizone blue shifts from 610 nm to 502 nm (dithizone–Hg^{2+} complex), the quenched red luminescence of $LaVO_4:Eu^{3+}$ NPs encapsulated in the nanocomposites was turned on. Meanwhile, other cations have no effects on the visual luminescence turn-on assay of Hg^{2+}. Therefore, we have successfully developed a facile and novel nanocomposite-based luminescence turn-on assay protocol for the rapid, visual, sensitive, and selective detection of mercury ions in aqueous media. This newly developed strategy will pave the way to the fabrication of luminescence turn-on nanosensors and draw wide attention in the field of biochemical sensing and environmental protection.

Acknowledgments

This research was supported in part by the National Natural Science Foundation of China (Grant Nos. 21275015 and 21075009), the State Key Project of Fundamental Research of China (Grant No. 2011CB932403), and the Program for New Century Excellent Talents in University of China (No. NCET-10-0213).

Appendix A. Supporting information

Supplementary data associated with this article can be found in the online version at http://dx.doi.org/10.1016/j.talanta.2013.05.069.

References

[1] F. Loe-Mie, G. Marchand, J. Berthier, N. Sarrut, M. Pucheault, M. Blanchard-Desce, F. Vinet, M. Vaultier, Angew. Chem. Int. Ed. 122 (2010) 434–437.
[2] P. Pallavicini, Y.A. Diaz-Fernandez, F. Foti, C. Mangano, S. Patroni, Chem.—Eur. J. 13 (2006) 178–187.
[3] X.P. Yan, X.B. Yin, D.Q. Jiang, X.W. He, Anal. Chem. 75 (2003) 1726–1732.
[4] C. Ma, F. Zeng, L.F. Huang, S.Z. Wu, J. Phys. Chem. B 115 (2011) 874–882.
[5] H. Li, L.Y. Wang, Analyst 138 (2013) 1589–1595.
[6] J. Canário, M. Caetano, C. Vale, Anal. Chim. Acta 580 (2006) 258–262.
[7] L.Q. Guo, N. Yin, D.D. Nie, J.R. Gan, M.J. Li, F.F. Fu, G.N. Chen, Analyst 136 (2011) 1632–1636.
[8] Y.K. Yang, K.J. Yook, J. Tae, J. Am. Chem. Soc. 127 (2005) 16760–16761.
[9] H. Zheng, Z.H. Qian, L. Xu, F.F. Yuan, L.D. Lan, J.G. Xu, Org. Lett. 8 (2006) 859–861.
[10] Y.M. Guo, Z. Wang, W.S. Qu, H.W. Shao, X.Y. Jiang, Biosens. Bioelectron. 26 (2011) 4064–4069.
[11] D.B. Liu, Z. Wang, X.Y. Jiang, Nanoscale 3 (2011) 1421–1433.
[12] X.Q. Chen, J. Jia, H.M. Ma, S.J. Wang, X.C. Wang, Anal. Chim. Acta 632 (2009) 9–14.
[13] J. Jia, K. Wang, W. Shi, S.M. Chen, X.H. Li, H.M. Ma, Chem.—Eur. J. 16 (2010) 6638–6643.
[14] W. Shi, S.N. Sun, X.H. Li, H.M. Ma, Inorg. Chem. 49 (2010) 1206–1210.
[15] Z. Gu, M.X. Zhao, Y.W. Sheng, L.A. Bentolila, Y. Tang, Anal. Chem. 83 (2011) 2324–2329.
[16] Y. Takahashi, S. Danwittayakul, T.M. Suzuki, Analyst 134 (2009) 1380–1385.
[17] L.N. Zhu, J.G. Qin, C.L. Yang, Chem. Commun. 46 (2010) 8755–8757.
[18] Z.L. Zhu, G.C.Y. Chan, S.J. Ray, X.R. Zhang, G.M. Hieftje, Anal. Chem. 80 (2008) 7043–7050.
[19] Z.B. Gao, X.G. Ma, Anal. Chim. Acta 702 (2011) 50–55.
[20] M. Rex, F.E. Hernandez, A.D. Campiglia, Anal. Chem. 78 (2006) 445–451.
[21] J.N. Wilson, U.H.F. Bunz, J. Am. Chem. Soc. 127 (2005) 4124–4125.
[22] Q. Liu, J.J. Peng, L.N. Sun, F.Y. Li, ACS Nano 5 (2011) 8040–8048.

[23] D. Li, S.P. Song, C.H Fan, Acc. Chem. Res. 43 (2010) 631–641.
[24] Z. Zhu, Y.Y. Su, J. Li, D. Li, J. Zhang, S. Song, Y. Zhao, G.X. Li, C.H Fan, Anal. Chem. 81 (2009) 7660–7666.
[25] M.L. Deng, Y.X. Ma, S. Huang, G.F. Hu, L.Y. Wang, Nano Res. 4 (2011) 685–694.
[26] R. Freeman, T. Finder, I. Willner, Angew. Chem. Int. Ed. 48 (2009) 7818–7821.
[27] B.Y. Han, J.P. Yuan, E.K. Wang, Anal. Chem. 81 (2009) 5569–5573.
[28] D.B. Liu, W.W. Chen, K. Sun, K. Deng, W. Zhang, Z. Wang, X.Y. Jiang, Angew. Chem. Int. Ed. 50 (2011) 4103–4107.
[29] L.T. Kong, J. Wang, G.C. Zheng, J.H. Liu, Chem. Commun. 47 (2011) 10389–10391.
[30] X. Wang, J. Zhuang, Q. Peng, Y.D. Li, Nature 437 (2005) 121–124.
[31] Y.X. Wang, J.S. Li, H. Wang, J.Y. Jin, J.H. Liu, K.M. Wang, W.H. Tan, R.H. Yang, Anal. Chem. 82 (2010) 6607–6612.
[32] F.Q. Zhang, L.Y. Zeng, C. Yang, J.W. Xin, H.Y. Wang, A.G. Wu, Analyst 136 (2011) 2825–2830.
[33] S. Huang, W. Yan, G.F. Hu, L.Y. Wang, J. Phys. Chem. C 116 (2012) 20558–20563.
[34] M. Zhang, M.X. Yu, F.Y. Li, M.W. Zhu, M.Y. Li, Y.H. Gao, L. Li, Z.Q. Liu, J.P. Zhang, D.Q. Zhang, T. Yi, C.H. Huang, J. Am. Chem. Soc. 129 (2007) 10322–10323.
[35] Q.A. Zhao, F.Y. Li, C.H. Huang, Chem. Soc. Rev. 39 (2010) 3007–3030.
[36] Z.Z. Lin, X.H. Li, H.B. Kraatz, Anal. Chem. 83 (2011) 6896–6901.
[37] J.W. Liu, Y. Lu, Angew. Chem. Int. Ed. 119 (2007) 7731–7734.
[38] A. Ono, H. Togashi, Angew. Chem. Int. Ed. 43 (2004) 4300–4302.
[39] H. Wang, Y.X. Wang, J.Y. Jin, R.H. Yang, Anal. Chem. 80 (2008) 9021–9028.
[40] L.B. Zhang, T. Li, B.L. Li, J. Li, E.K. Wang, Chem. Commun. 46 (2010) 1476–1478.
[41] Z.D. Wang, J.H. Lee, Y. Lu, Chem. Commun. 45 (2008) 6005–6007.
[42] M. Famulok, G. Mayer, M. Blind, Accounts Chem. Res. 33 (2000) 591–599.
[43] N. Dave, M.Y. Chan, P.J.J. Huang, B.D. Smith, J.W. Liu, J. Am. Chem. Soc. 132 (2010) 12668–12673.
[44] A.A. Ansari, M. Alam, J.P. Labis, S.A Alrokayan, G. Shafi, T.N Hasan, N.A Syed, A. A. Alshatwi, J. Mater. Chem. 21 (2011) 19310–19316.
[45] C.J. Jia, L.D. Sun, L.P. You, X.C. Jiang, F. Luo, Y.C. Pang, C.H. Yan, J. Phys. Chem. B 109 (2005) 3284–3290.
[46] G.C. Liu, X.C. Duan, H.B. Li, H. Dong, Mater. Chem. Phys. 115 (2009) 165–171.
[47] S. Setua, D. Menon, A. Asok, S. Nair, M. Koyakutty, Biomaterials 31 (2010) 714–729.
[48] M.S. Hosseini, H. Hashemi-Moghaddam, Talanta 67 (2005) 555–559.
[49] N. Rajesh, G. Gurulakshmanan, Spectrochim. Acta A 69 (2008) 391–395.
[50] N. Rajesh, M.S. Hari, Spectrochim. Acta A 70 (2008) 1104–1108.
[51] A. Safavi, M. Bagheri, Sens. Actuator B-Chem. 99 (2004) 608–612.
[52] M.J. Shaw, P. Jones, P.R. Haddad, Analyst 128 (2003) 1209–1212.
[53] Y.G. Yin, M. Chen, J.F. Peng, J.F. Liu, G.B. Jiang, Talanta 81 (2010) 1788–1792.
[54] F. Bai, D.S. Wang, Z.Y. Huo, W. Chen, L.P. Liu, X. Liang, C. Chen, X. Wang, Q. Peng, Y.D. Li, Angew. Chem. Int. Ed. 46 (2007) 6650–6653.
[55] Y.X. Ma, H. Li, S. Peng, L.Y. Wang, Anal. Chem. 84 (2012) 8415–8421.
[56] Y.X. Ma, H. Li, L.Y. Wang, J. Mater. Chem. 22 (2012) 18761–18767.
[57] Y.Y. Zhao, Y.X. Ma, H. Li, L.Y. Wang, Anal. Chem. (2012)5447.
[58] H. Li, H.J. Wang, L.Y. Wang, J. Mater. Chem. C 1 (2013) 1105–1110.
[59] L.Y. Wang, P. Li, Y.D. Li, Adv. Mater. 19 (2007) 3304–3307.
[60] L.Y. Wang, R.X. Yan, Z.Y. Hao, L. Wang, J.H. Zeng, H. Bao, X. Wang, Q. Peng, Y. D. Li, Angew. Chem. Int. Ed. 44 (2005) 6054–6057.
[61] M.L. Deng, N.N. Tu, F. Bai, L.Y. Wang, Chem. Mater. 24 (2012) 2592–2597.
[62] L.Y. Wang, Y.D. Li, Chem. Mater. 19 (2007) 727–734.
[63] C. Yuan, K. Zhang, Z.P. Zhang, S.H. Wang, Anal. Chem. 84 (2012) 9792–9801.
[64] M.Y. An, J.B. Cui, Q. He, L.Y. Wang, J. Mater. Chem. B 1 (2013) 1333–1339.
[65] J.F. Liu, Y.D. Li, Adv. Mater. 19 (2007) 1118–1122.
[66] J.F. Liu, Y.D. Li, J. Mater. Chem. 17 (2007) 1797–1803.